

# Improved Electrical Conductivity and Strength of $\alpha$ -Al-Carbon Nanotubes Blended with Silver Nanoparticles Composites

V. S. Aigbodion<sup>1, 2, 3\*</sup>

<sup>1</sup>Africa Centre of Excellence, ACESPED University of Nigeria, Nsukka, Nigeria

<sup>2</sup>Department of Metallurgical and Materials Engineering, University of Nigeria, Nsukka, Nigeria

<sup>3</sup>Faculty of Engineering and Built Environment, University of Johannesburg, P. O. Box 534, Auckland Park, South Africa



**ABSTRACT:** An attempt has been made to develop a new enhanced electrical conductor nanocomposites using green synthesis silver nanoparticles (GAgNPs) modified carbon nanotubes (CNTs) reinforced aluminum nanocomposites. High-intensity ball milling and spark plasma sintering (SPS) were used to produce the composites. The nanocomposite' microstructure, strength, model, and electrical conductivity were all determined. 2% GAg.NPs in Al-4-percent CNTs helps to refine the grain structure of the Al-4-percent CNTs. More dislocation density was generated by the creation of sub-grain in the Al-4 percent CNTs+2 percent GAgNPs composite. Tensile strength and electrical conductivity were increased by 82.14 and 106.88% using Al-4-percent CNTs +2%GAg.NPs nanocomposite. The ductility mode of fracture associated with the tiny sub-grain produced at the surface was greatly improved when 2% GAgNPs were added to Al-4% CNTs. It was established that the GAgNPS can be used to coat CNTs enhance the strength and electrical conductivity of Al-4 percent CNTs nanocomposites.

**KEYWORDS:** Nanoparticles, Cashew leaves, Electrical conductivity, Microstructure, Strength analysis, Composites

[Received May 28, 2022; Revised Jul. 8, 2022; Accepted Jul. 19, 2022]

Print ISSN: 0189-9546 | Online ISSN: 2437-2110

## I. INTRODUCTION

Aluminum has been utilized to make electrical wires for overhead transmission for many years Guo *et al.*, (2017), Ujah *et al.*, (2020a), Ujah *et al.*, (2019a), Mohammed *et al.*, (2020). Aluminum hardness values, low temperature and strength, on the other hand, limited its employment in applications requiring great strength and heat (Sharma and Sharma, (2014); Chiang *et al.*, (2001); Park *et al.*, (2019). Many researches have into improving the strength and electrical conductivity of aluminum conductor Bandaru, (2007). The researchers chose to work with aluminum because of its high electrical conductivity Zhao *et al.*, (2019). They discovered that the composites have the potential to be used for high-strength overhead transmission wires. Carbon nanotube (CNTs) is one of the nanoparticles' electrical conductive reinforcements that are catching researchers' interest for improving the electrical conductivity of Al due to its high electrical conductivity Dujardin *et al.*, (1994).

CNTs have been effectively employed to enhance the conductive properties of Al-CNTs Jyoti *et al.*, (2016), Zhang *et al.*, (2019). Microstructure, wear characteristics, and electrical conductivity of Al-CNTs produced by SPS were studied by Ujah *et al.* (2019b). They noticed the overhead transmission conductor's exceptional electrical conductivity, thermal qualities, and wear resistance. In their work, Mansoor and Shahid (2016) produced carbon nanotube reinforced aluminium composite (Al-CNTs) using the induction melting

process. Results showed that the yield increased significantly by 77% while tensile strength increased by 52%. In spite of CNTs' having high thermal characteristics and electrical conductivity, their high cost of production and de-entanglement restricted their usage in electronic devices Shin *et al.*, (2015); Dujardin *et al.*, (1994). To improve dispersion in the aluminum matrix, a large shear force is normally required to overcome this constraint So *et al.*, (2011). Wet mixing, metallic nanoparticles and ultrasonic cavitation have been employed to improve CNTs dispersion in aluminum Simes *et al.*, (2015); Kawecki *et al.*, (2016), Choi *et al.*, (2005). However, long time of wet mixing and ultrasonic cavitation results to work hardening of the nanoparticles and decreased the ductility and formability of the powders Kawecki *et al.*, (2016).

In recent times, studies have been devoted to using metal nanoparticles in the modification of CNTs for high magnetic, optical and electrical properties. However, silver nanoparticles (Ag.NPs) modified CNTs have received great attention as a result of their potential applications as electrical conductivity, catalysts, advanced materials, and optical limiters Ujah *et al.*, (2019c). Irhayyim *et al.* (2019) conducted a study to examine the mechanical performance of micro-Cu and nano-Ag reinforced Al-CNTs composite. Powder metallurgy technique was used to blend Ag NPs and Cu in percentages of 1, 2, or 3.4% with Al-1 percent CNTs so as to strengthen it. The compressive strength, microstructure, and hardness values of the composite were determined. They observed optimum at

\*Corresponding author: victor.aigbodion@unn.edu.ng

Al-1%CNTs+%2Ag NPs. The usage of Ag-nanoparticles to enhance the electrical conductivity of Al/CNTs has been shown to be promising the literature. However, the high cost of silver compared to CNTs further limits the usage of Ag nanoparticles to enhance CNTS Zhang *et al.*, (2019). Hence, there is an urgent need to develop silver nanoparticles from biosynthesis and reduce the cost of Ag-nanoparticles used in the enhancement dispersion of CNTs in aluminum matrix. The present work synthesized Ag-nanoparticles using cashew leaf extract to enhance the strength and conductivity of Al-CNTs composites. Cashew leaves have been reported to serve as antimicrobial agents for the reduction of Ag+ to Ag Arintonang *et al.*, (2019), Hemlata *et al.*, (2020), Ahmed *et al.*, (2020), Ujah *et al.*, (2019d). The utilization of cashew leaf extract to synthesize Ag-nanoparticles will be eco-friendly and cost-effective. Hence, this work will report for the first time the electrical conductivity and fracture toughness of Al-CNTs modified with biosynthesized Ag-nanoparticle.

## II. METHODOLOGY

Aluminum powder of 99.98% purity used in this work was purchased in Lagos, Nigeria. CNTs with an internal central diameter of 5–10nm and external diameters of 10–40nm were purchased in China (Hongwu International Group of Companies) (Figures 1a and 1b) was used in this work. The carbon layers that made up the CNT walls were virtually straight, parallel to one another, and inclined at an angle of around 45 degrees.

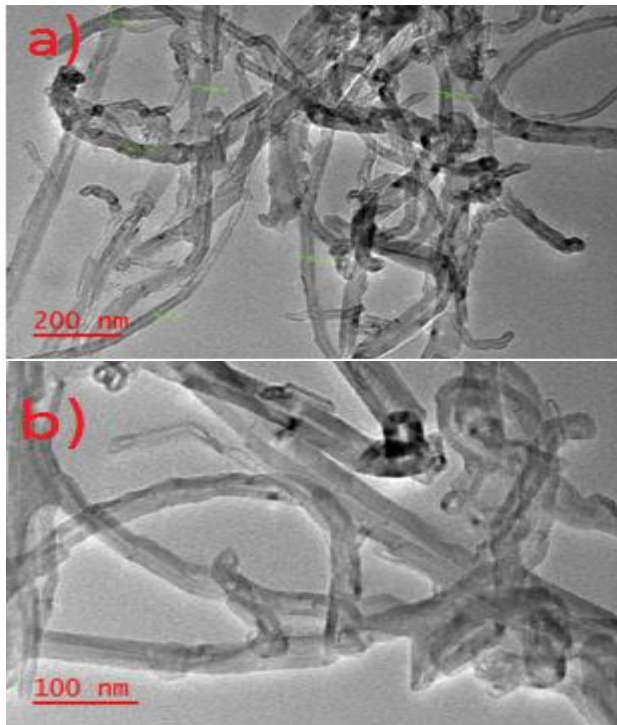


Figure 1: (a) TEM image of CNTs at 200nm (b) TEM image of CNTs at 100nm.

Fresh cashew leaves utilized in this study were obtained from the University of Nigeria, Nsukka, Nigeria. The fresh leaves were cleaned with distilled water and dried. Afterward

a solution of AgNO<sub>3</sub> (100ml) was added to the cleaned cashew leaves and soaked for an hour. A colour change from yellow to dark brown solution was observed, and the solution was heated at temperature 100 °C at a stirring speed of 2000 rpm. Then centrifugation was used to obtain solid GAgNPs. Functionalisation of the CNTs was done using a mixture of 30% H<sub>2</sub>O<sub>2</sub> and 65% HNO<sub>3</sub> and filtered, HAAK Rheomix with a model number of 600 OS made by Thermo Electron Company USA was used. The filtrate was diluted with water to reduce the pH to 7. To generate carboxylic acid-functionalised CNTs, H<sub>2</sub>O<sub>2</sub> was added Bastwros *et al.*, (2013), Yuan, (2018). Tencanspeed vibrating ball mill, Tianchuang Powder Technology Co., Lt. Changsha was used to ball mill Al-x%CNTs (x=1, 2, 3, 4)+2% GANPs. The ball milling was done using fifty (50) tungsten balls, 10 mm diameter inside, speed of 300 rpm and for 2hours. The goal was to ensure that the reinforcements were evenly distributed throughout the aluminum matrix. Composition utilized in the paper was selected following preliminary research and in agreement with the findings of Zhang *et al* (2019). Microstructure and particle size of AgNPs and blended GAgNPs+CNTs were determined by Jeol JEM-2100F, transmission electron microscopy (TEM). JEOL Ltd., USA products.

Composites were produced using the SPS model SPS10-3, Henan Zg Industrial Products Co.,Ltd China. SPS is made up of a furnace, cooling/vacuum units, and a power section. For the sintering, a voltage of 5V and a current of 300amps were employed. Composites were produced using Al-x%CNTs (where x=1, 2, 3, 4) with 2% GAgNPs addition. Formulation blend was pressed onto a graphite mold of 100 mm in diameter using a pressure of 50 MPa. The sintering was done at a temperature of 580 °C with a heating rate of 10 °C/min. Cutting of the samples was done with an automated cutting machine (model: Robofill240) Zhejiang Guowei Intelligent Equipment Co., Ltd. Electrical conductivity was done using a Kaise tester, model SK5010, Kaise Ltd USA. Electrical conductivity of the samples was computed using Eqn. (1) (Yuan, 2018).

$$\sigma = \frac{1}{\rho} = \frac{d}{(R_p)A} \quad (1)$$

where:  $A$  = area,  $d$  = thickness, and  $\rho$  = electrical resistance,  $\sigma$  = electrical conductivity,  $R_p$  = Resistivity

VEGA 3 TESCAN Scanning electron microscopy, Tescan Orsay Holding Czech Republic manufacturer was used to determine the microstructure of the samples. Testometric universal testing, Testometric Co, United Kingdom was used to determine the tensile strength in accordance with ASTM D3039 standard. A sample size of 5 mm x 10 mm x 60 mm and crosshead speed was 1 mm/min were employed for the tensile test. Autodesk software was employed for the stress analysis of the sample.

## III. RESULTS AND DISCUSSION

### A. TEM Analysis

Figure 2 shows the results of the TEM imaging of the produced GAgNPs. It was observed circular and spherical shape was viewed in the TEM image of the GAgNPs. Microstructure of the composite microstructure exhibits well-

distributed nanoparticles with little clumping. Particle size ranged from 45 to 65 nanometers. Ag element has greater peaks in the EDS. The quality of the Ag NPs produced was good, since the EDS revealed no oxygen or silver compound formation. A similar observation was reached by Hemlata *et al.*, (2020).

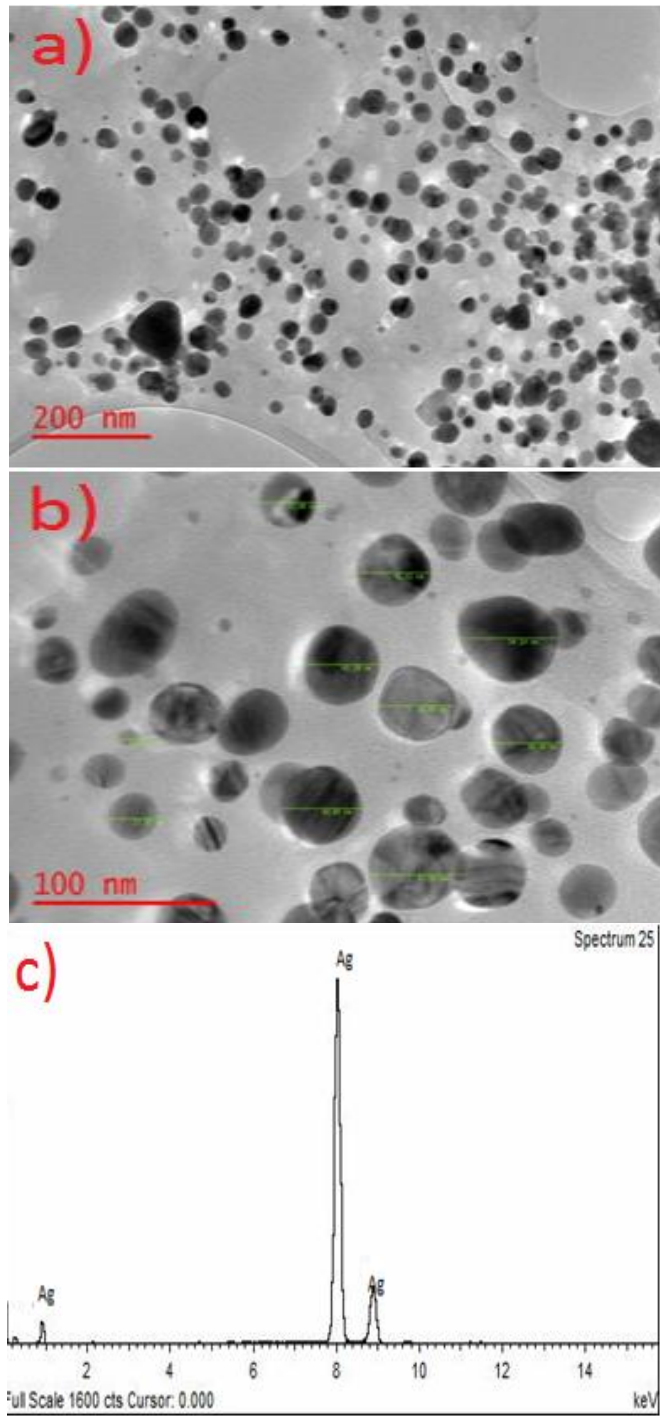


Figure 2: (a) TEM/ image of Ag NPs at 200nm (b) TEM/ image of Ag NPs at 100 nm (c) EDS spectrum of Ag NPs.

Figure 3 shows the SEM image of blended Al-4 percent CNTs-2 percent Gag NPs after wet mixing and high-intensity ball milling. It was observed that CNTs and Gag NPs were

found to be evenly and well disseminated in the Al-matrix, with of evidence little agglomeration. This was accomplished by combining the effects of wet mixing with ball milling.

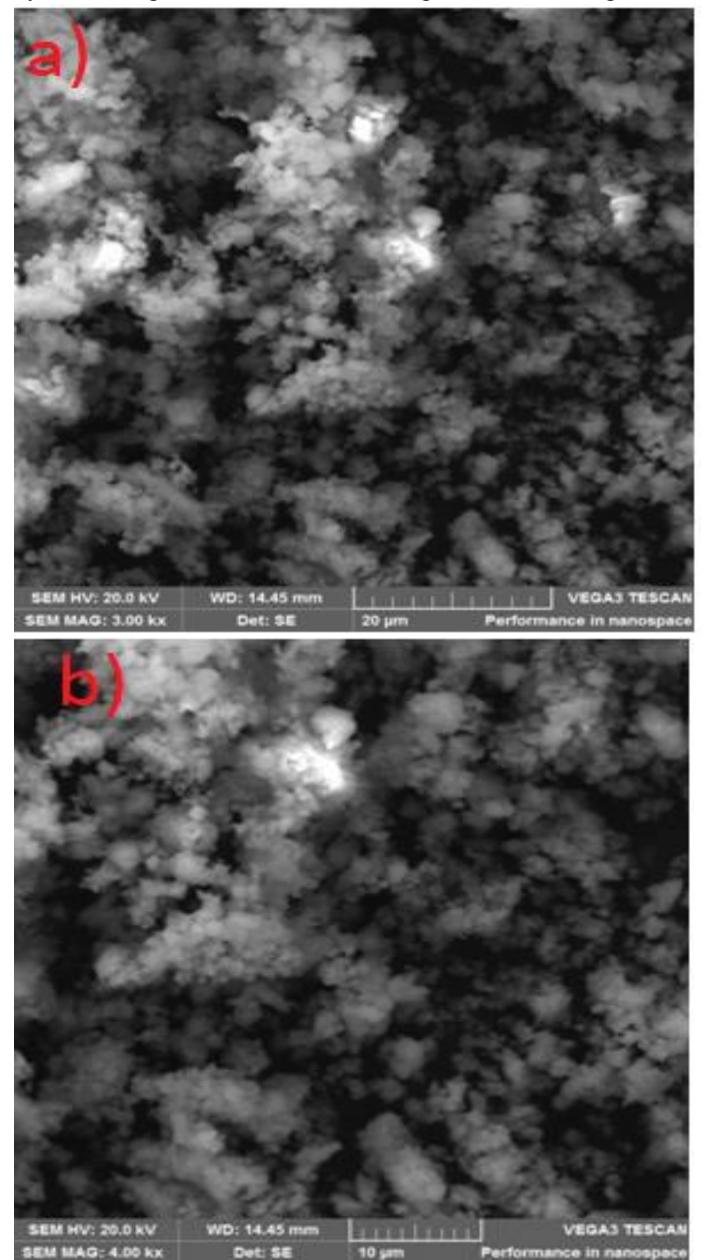
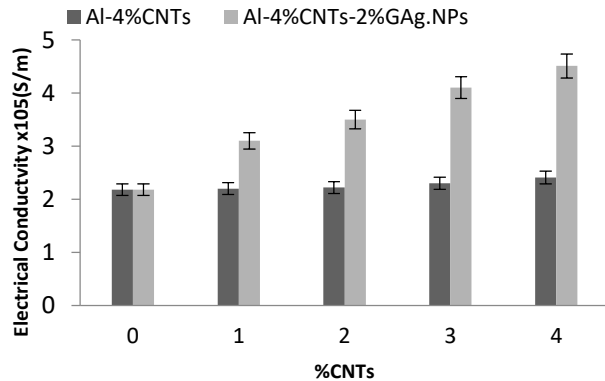


Figure 3: (a) SEM image of Al-4%CNTs+2%GAgNPs at 3000k magnification (b) SEM image of Al-4%CNTs+2%GAgNPs at 4000k magnification.

### B. Electrical Conductivity

The findings for electrical conductivity are shown in Figure 4. It was found that the electrical conductivity of the samples were significantly improved. The electrical conductivity increased with the rise of the CNTs and GAgNPs in the formulation. The electrical conductivity of the Al was improved by adding CNTs and GAgNPs. Pure Al has an electrical conductivity of  $2.18 \times 10^5$  S/m as obtained from literature Selvakumar *et al.*, (2016). The combination of carbon nanotubes (CNTs) and silver nanoparticles (GAgNPs+CNTs) has a significant impact on electrical conductivity. The

electrical conductivity of Al-nanocomposites rose as the CNT content in the formulation increased (Figure 4). However the Al-GAgNPs+CNTs nanocomposites have a larger increment in electrical conductivity than the Al-CNTs nanocomposites. This was attributed to the fact that GAgNPs conduct electricity better than aluminum. This finding was at par with the work of Guillon, (2020).



**Figure 4:** Variation of Electrical Conductivity of the samples with %CNTs.

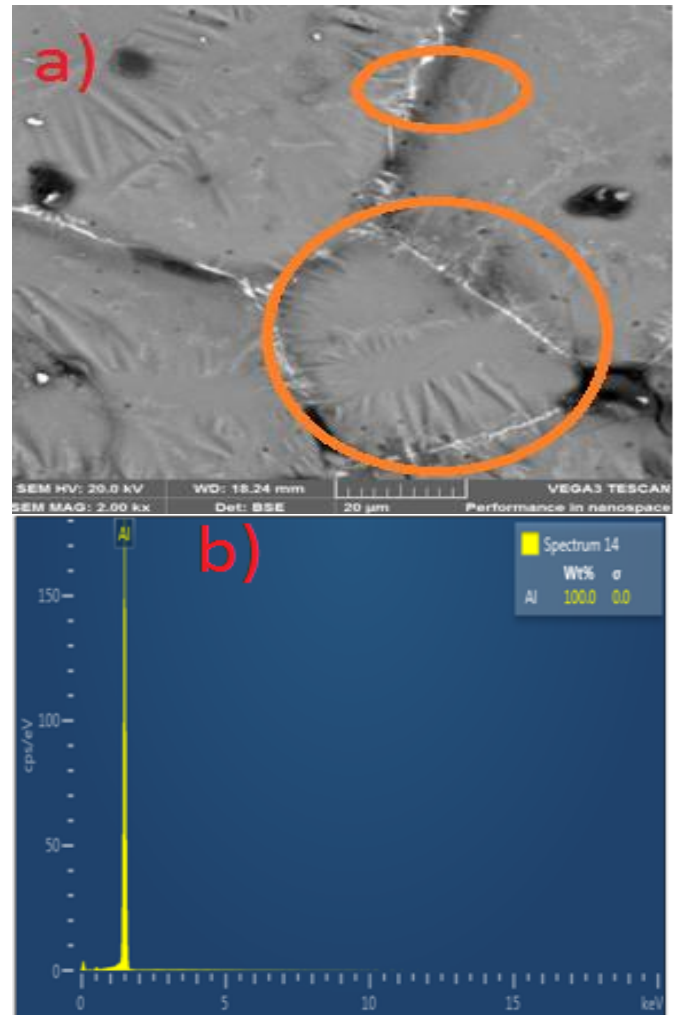
The increment of the electrical conductivity of Al-2%GAgNPs+CNTs composite than that of Al-CNTs was attributed to a better dispersion of the CNTs in the Al-matrix and lead to high-aspect-ratio of the conductive pathways of the sample. The electrical conductivity of the Al-matrix increased from  $2.18 \times 10^5 \text{S/cm}$  to  $2.41 \times 10^5 \text{S/cm}$  for Al-4%CNTs and  $4.51 \times 10^5 \text{S/cm}$  for Al-4%CNTs-2%GAgNPs and corresponded to 10.55% and 106.88% enhancements in the electrical conductivity of the samples. The results obtained in this work are higher than the work of Ujah *et al.* (2019e).

### C. SEM Analysis

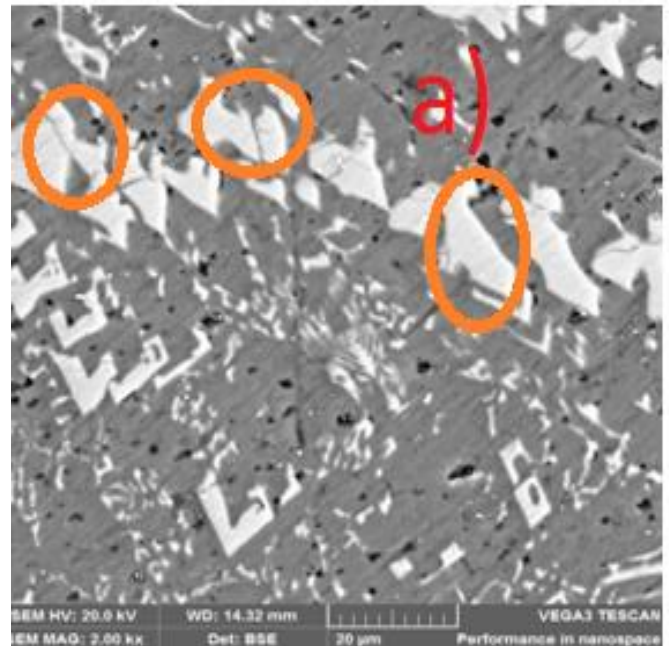
Figures 5 to 7 show the new structure generated after sintering was determined using SEM. It was observed that the formation of new grain with the addition of GAgNPs and CNTs was the major reason for the morphological changes in Figure 5a and Figures 6a-7a. Reinforcing phases are shown as the whitish colour as dotted with circles in Figures 6-7, while the grey colour represents the Al-matrix phases. In Figure 5a the  $\alpha$ -Al structure with a large grain boundary was evident in the microstructure of the matrix. However, in Figure 7a the addition of GAgNPs results in the formation of a smaller sub-grain in the SEM of the Al-4% CNTs+2%GAgNPs as compared with the Al-4%CNTs composite in Figure 6a. This sub-grain may increase the dislocation density of the Al-4% CNTs+2%GAgNPs and enhance the strength and electrical conductivity of the developed composites.

From Figure 5b the high peak of Al in the EDS of the aluminum matrix confirms with the prior finding that the aluminum employed in this study contain high parentage of Al. Figure 6b shows the presence of C and Al in the EDS of the Al-4%CNTs composite, while C, Ag, and Al was seen in the EDS of the Al-4%CNTs+2%GAgNPs. The absence of oxygen in this study suggests that there was no brittleness and debonding of the developed composites. This was made

possible because of the use of SPS. Similar observation reported in the work of Ujah *et al.* (2019c).



**Figure 5:** (a) SEM image of the Al-matrix (b) EDS spectrum of the Al-matrix.



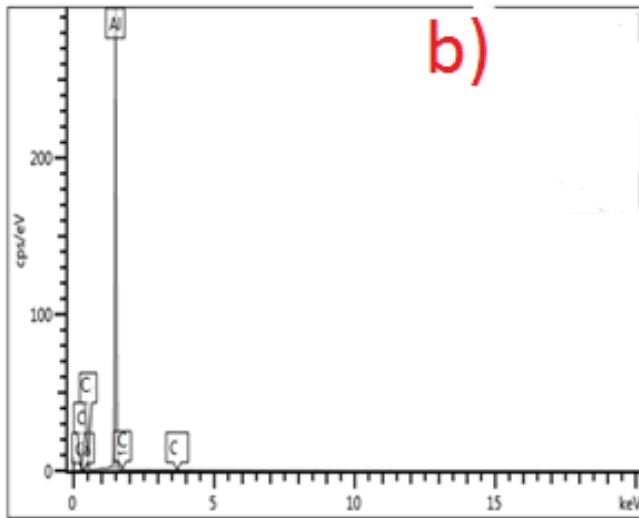


Figure 6: (a) SEM image of the Al-4%CNTs composite (b) EDS spectrum of the Al-4%CNTs composite.

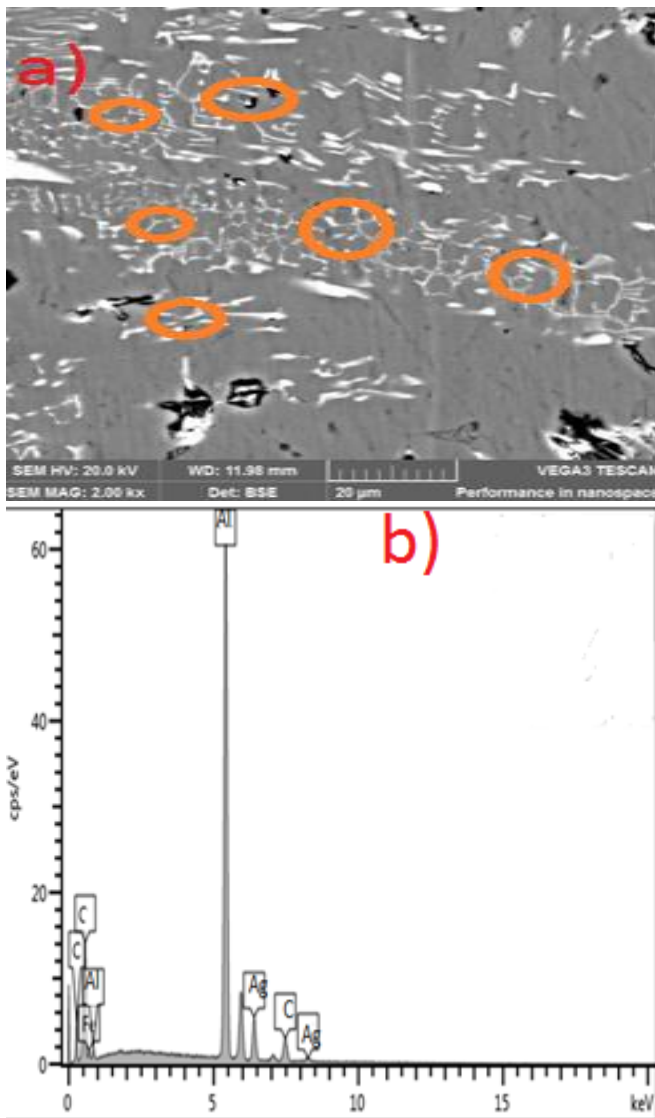


Figure 7: (a) SEM image of the Al-4%CNTs-2%GAg.NPs composite (b) EDS spectrum of the Al-4%CNTs-2%GAg.NPs composite.

D. Tensile Strength

Figure 8 shows the stress-strain curves derived from the samples under investigation. Composites have a larger area under the stress-strain curve than pure aluminum, as seen in Figures 8 a, b and c. These show that the Al-4%CNTs, and Al-4 percent CNTs+2%GAgNPs nanocomposites are tougher and absorb high energy before fracture than pure Al based matrix. Al-4%CNTs, and Al-4 percent CNTs+2%GAgNPs composites' have greater tensile strength and elastic modulus this shows that the reinforcing phases were successful used in increasing the strength of the Al-matrix. However, Al-4%CNTs+2%GAgNPs samples have the greatest strength of all sample, for example a tensile strengths of 113.43, 157.70, and 206.60 MPa were obtained for the Al-matrix, Al-4%CNTs, and Al-4 percent CNTs+2%GAgNP, respectively (Table 1), corresponding to an 82.14 percent increase in tensile strength of the pure Al when compared with Al-4%CNTs+2%GAgNPs. The creation of sub-grain helps generate greater dislocation density, this given by Eqns. 2 to 4 Ujah *et al.*, (2019c).

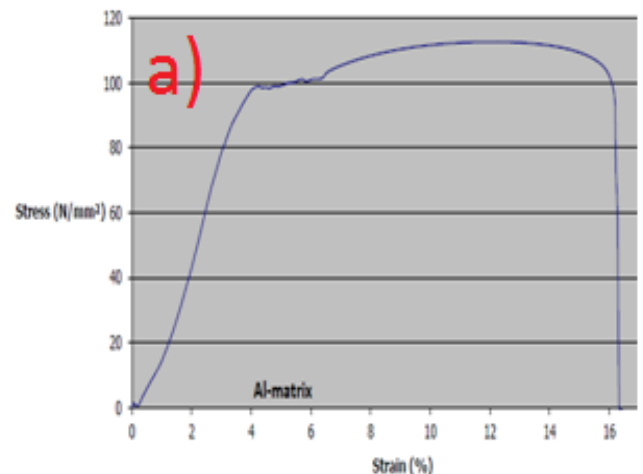
$$D_s = d \left( \frac{\pi d^2}{6 \phi_p} \right)^{1/2} \tag{2}$$

$$\Delta \sigma_{SKG} = k_{Y2} \cdot D_s^{-1/2} \tag{3}$$

$$\Delta \sigma_\alpha = \alpha \cdot G \cdot b \cdot \rho^{1/2} \tag{4}$$

Where: SKG denotes yield strength due to grain size,  $\rho$ = dislocation density,  $b$ = Burger's vector,  $p$ =particle size,  $D_s$ =sub-grain size,  $d$ =grain size,  $G$ =shear modulus,  $k_{Y2}$  constant ( $0.05 \text{ MN m}^{-3/2}$ ),  $p$ =particle content, and = yield strength.

The higher the sub-grain and grain size results in an increment in dislocation density as given by Eqn. 2 and hence leads to an increment in the yield strength of the composites as given by Eqns. 3 to 4. Dislocation density may prevent from freely moving grain along the grain boundary, thereby increasing the matrix's strength. Researchers, Ujah *et al.*, (2020a), Mohammed *et al* (2020) have reported similar increase in dislocation density of due to Al- particle strengthen. It may be inferred that the produced Al-4 percent CNTs+2%GAgNPs nanocomposite can be used to create a higher-strength conductor.



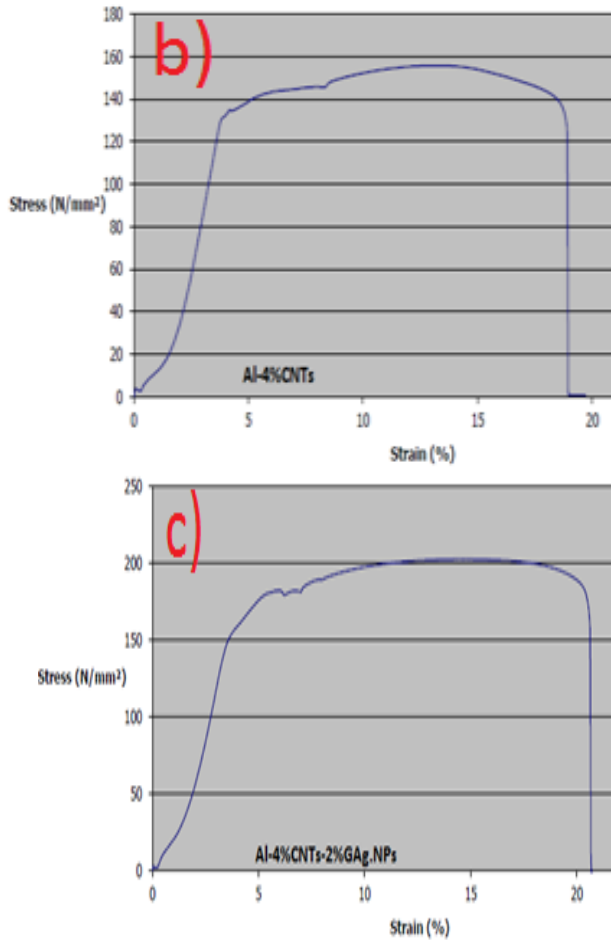


**Figure 8:** stress versus strain curves of a) Al-matrix b) Al-4%CNTs c) Al-4%CNTs-2%GAg.NPs

EM is for elastic modulus, YS stands for yield strength, TS stands for tensile strength, SB stands for strain at break, EB stands for energy at the break, and ELB stands for elongation at break.

#### 1) Tensile SEM fracture analysis

Figure 9a shows the fracture mechanism of the  $\alpha$ -Al which consisted of a combination of brittle-ductile fractures with rips, edges, and transgranular cleavage Nilagiri *et al.*, (2018). The developed nanocomposites have different fracture modes from the  $\alpha$ -Al. Figure 9b shows the fracture image of the Al-4%CNTs nanocomposite intercrystalline carbon particles without delamination of the particles at interfaces were seen. These findings are in consistent with the work of Ujah *et al.*, (2020a). In Figure 9c the Al-4%CNTs+2%GAgNPs revealed

an improved ductility mode of fracture, which can be attributed to the tiny sub-grain generated in the sample. Fairly homogeneously distributed GAgNPs-CNTs improve the composite resistance to fractures under load. Because the CNTs modified with GAgNPs allows the ease transmission of load from the matrix to the reinforcement Ujah *et al.* (2020a). Also the fairly interfacial between the CNTs and GAg.NPs, observed in the SEM image in Figure 7 prevent the pulled out of GAgNPs-CNTs from the Al matrix as can be seen clearly in the SEM image of the Al-4%CNTs+2%GAgNPs composite.

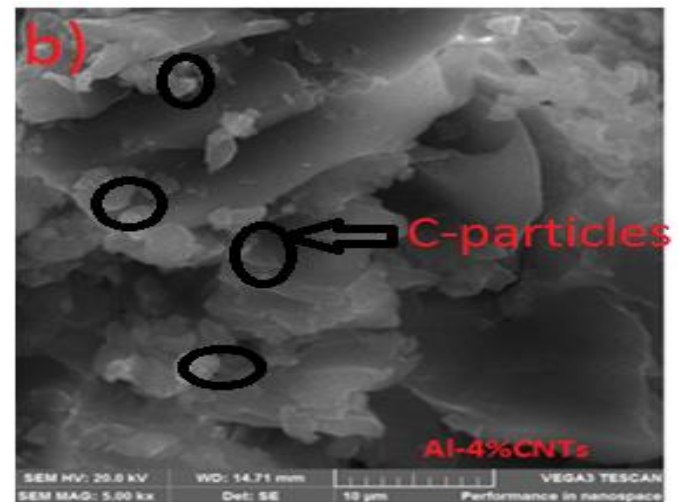
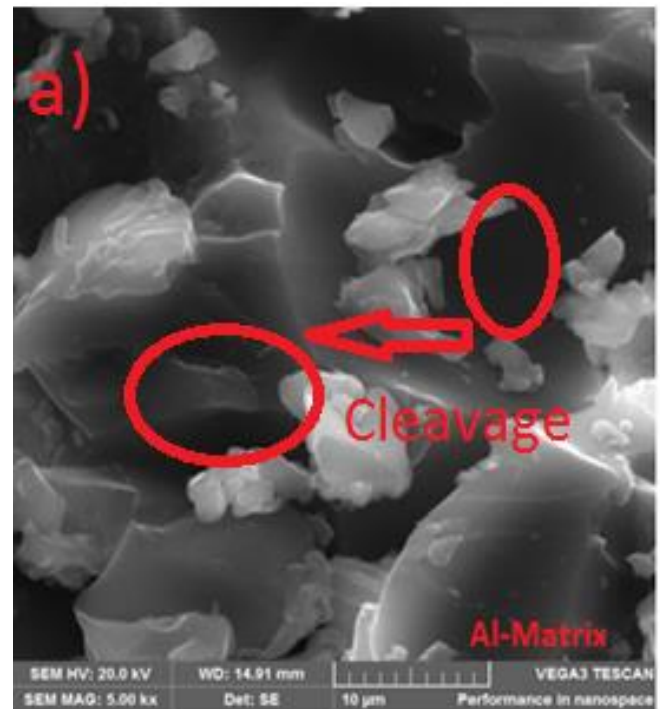


**Table 1: Results of the tensile properties.**

Samples	EM(MPa)	YS(MPa)	TS(MPa)	SB(%)	EB(N.M)	ELB(mm)
Al-matrix	2891.34	98.57	113.43	16.46	356.89	28.45
Al-4%CNTs	3987.21	143.56	157.70	19.70	598.26	35.68
Al-4%CNTs-2%GAg.NPs	4890.35	198.50	206.80	20.78	639.56	38.89

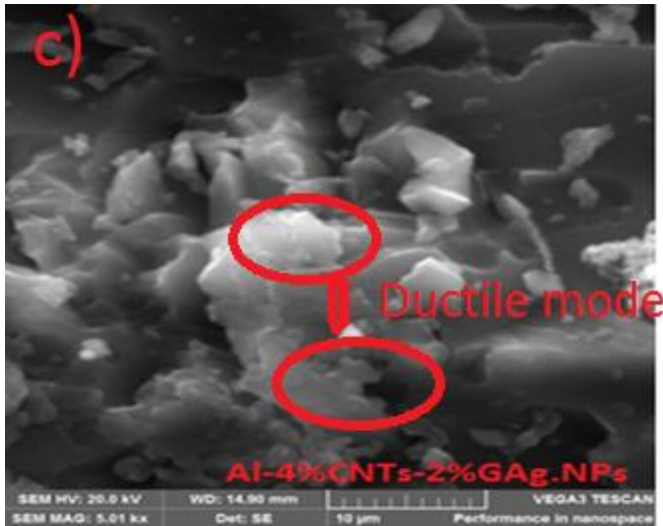


Figure 9: Fracture surface of a)Al-matrix b)Al-4%CNTs c) Al-4%CNTs-2%GAg.NPs.

2) Stress analysis of the samples

Equations 5 to 7 were used to compute the equivalent strain, displacement, Von Mises stress, and factor of safety for the stress analysis. The Al-4%CNTs+2% GAgNPs as subjected to a tensile stress of 2000 N, as recommended for high tension conductor applications Ujah *et al.* (2020a). The mechanical characteristics for the simulation were taken from Table 1. The force and moments of the system are shown in Table 2. The displacement in the x and z directions and the center position of the y-displacement were used as the boundary conditions. In order to choose the mesh that offers a high accuracy and a reasonable computing cost, a mesh sensitivity research was conducted. For the mesh sensitivity study, a 0.2 minimum element size, 0.1 average element size, maximum angle of 60 degrees, 0.1% model diameter, 0.05 shells, and 1.5 grading factor were used for the meshing.

$$\sigma_v = [0.5((\sigma_1 - \sigma_2)^2 + (\sigma_2 - \sigma_3)^2 + (\sigma_3 - \sigma_1)^2)]^{0.5} \quad (5)$$

$$EqS = \left(\frac{4}{3} \cdot \sigma_v\right)^{0.5} \quad (6)$$

$$F_s = \frac{\sigma_v}{W_s} \quad (7)$$

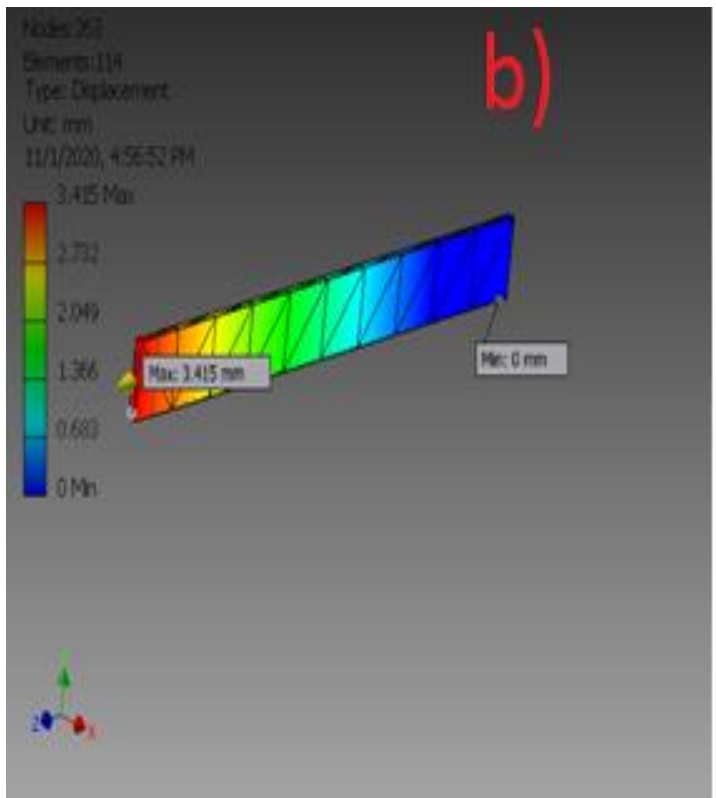
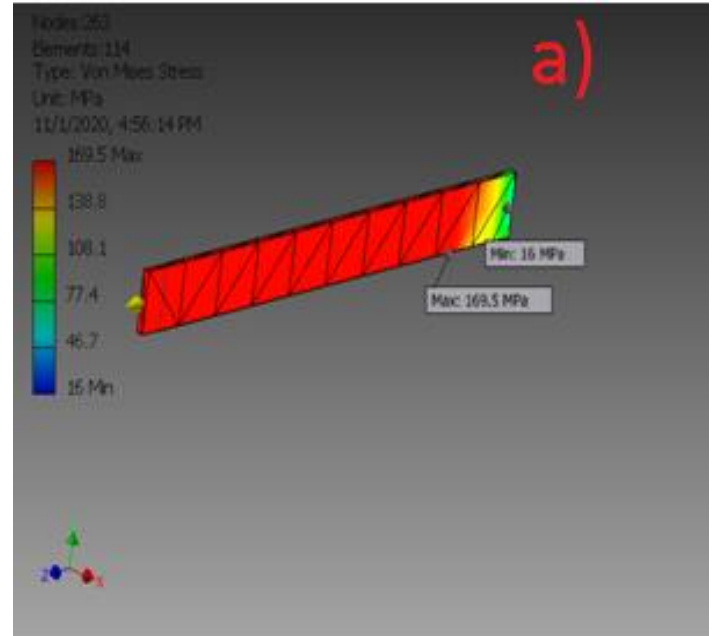
where:  $\sigma_v$  = Von mises stress,  $\sigma_1 \sigma_2 \sigma_3$  = principal stresses,  $EqS$  = Equivalent strain,  $W_s$  = workable stress,  $F_s$  = factor of safety.

Table 2: Reaction force and moment on constraints.

Constraint Name	Reaction Force		Reaction Moment	
	Magnitude	Component (X,Y,Z)	Magnitude	Component (X,Y,Z)
Fixed Constraint	2000N	0N	0.0108395	0N
		0N		0N
		-2000N		-0.0108395 N m

The findings of the stress study is given in Table 3, while the plots obtained in the stress analysis is shows in Figure 10. The Von Mises stress has a range of 15.9598 MPa to 169.547 MPa. When the forces were applied to the sample before deformation, the displacement and strain distribution were

measured in millimeters. The strain values ranged from 0.00348041 to 0.0344434. In this stress analysis study of the composite, the maximum displacement value was 3.41519 mm, the factor of safety was 1.17047 and 12.4343 and 169.547 MPa as Von Mises stress. The results of the Von Mises stress are lower than the sample yield strength as documented in Table 1. This indicates that utilizing this material for high-tension conductor’s results in a 1.17047 minimum factor of safety. The high strength and low safety factor are within the acceptable limit for tension conductor applications Ujah *et al.* (2020c), Zhao *et al.* (2019).



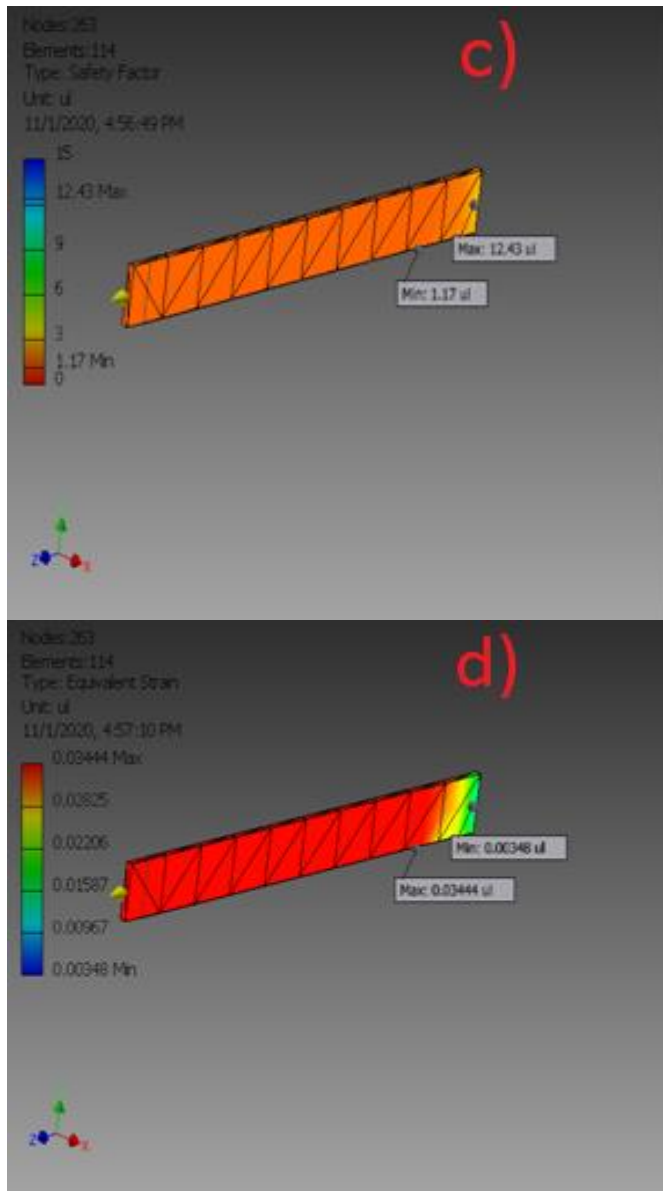


**Figure 10:** Stress analysis of the tensile strength (a) Von Mises stress (b) Displacement (c) Safety factor (d) strain.

**Table 3: Stress analysis of the simulation.**

Name	Minimum	Minimum
Displacement	0mm	3.41519 mm
Von Misses Stress	15.9598 MPa	169.547 MPa
Safety Factor	1.17047 ul	12.4343 ul
Equivalent Strain	0.00348041 ul	0.0344434 ul

#### IV. CONCLUSION

New information has been obtained in the modification of CNTs with green synthesized silver nanoparticles for the production of Al-CNTs+GAgNPs, in the course of the study the following conclusions are made: GAgNPs was successfully used in the modification of CNTs for enhanced dispersion in Al-matrix. Addition of 2% GAgNPs to Al-CNTs results to high dislocation density, formation of sub-grain and improved ductility mode of fracture, which can be attributed to the tiny sub-grain generated in the sample with 106.88 and 82.14%

increment in electrical conductivity and strength. The high strength and low safety factor obtained are within the acceptable limit for tension conductor applications. It has been estimated that a low-cost Ag-nanoparticle synthesized from cashew can be used for the enhancement of dispersion of CNTs in Al-matrix for the enhancement of electrical conductivity and strength.

#### ACKNOWLEDGMENTS

The author hereby appreciates and acknowledges the Africa Centre of Excellence for Sustainable Power and Energy Development (ACE-SPED) University of Nigeria, Nsukka, Energy Materials Research Group, University of Nigeria, Nsukka, Nigeria, and the Faculty of Engineering and Built Environment, University of Johannesburg, Auckland Park, South Africa for their support.

#### CONFLICTS OF INTEREST

The author declares no conflict of interest.

#### REFERENCES

- Ahmed, S. S; M. Ahmad; B. L. Swami and S. Ikram. (2016).** Green synthesis of silver nanoparticles using *Azadirachta indica* aqueous leaf extract. *Journal of Radiation Research and Applied Sciences*, (9), 1-7, <https://doi.org/10.1016/j.jrras.2015.06.006>.
- Aritonang, H.F.; H. Koleangan and A.D.Wuntu. (2019).** Synthesis of Silver Nanoparticles Using Aqueous Extract of Medicinal Plants' (*Impatiens balsamina* and *Lantana camara*) Fresh Leaves and Analysis of Antimicrobial Activity. *Int. J. Microbiol.*, 8642303, <https://doi.org/10.1155/2019/8642303>.
- Bandaru, P.R (2007):** Electrical Properties and Applications of Carbon Nanotube Structures. *Journal of Nanoscience and Nanotechnology*, (7), 1239-1267, <https://doi.org/10.1166/jnn.2007.307>.
- Bastwros, M.M.H.; A.M.K. Esawi and A. Wifi. (2013).** Friction and wear behavior of Al-CNTs composites. *Wear* (307), 164-173, <https://doi.org/10.1016/j.wear.2013.08.021>.
- Chiang, I.W.; B.E. Brinson; R.E.Smalley; J.L.Margrave and R.H.Hauge. (2001).** Purification and Characterization of Single-Wall Carbon Nanotubes. *The Journal of Physical Chemistry*, (105), 1157-1161, <https://doi.org/10.1021/jp003453z>.
- Choi, T.Y.; D. Poulikakos; J. Tharian and U. Sennhauser. (2005).** Measurement of thermal conductivity of individual multiwalled carbon nanotubes by the 3- $\omega$  method. *Applied Physics Letters* (87), 013108, <https://doi.org/10.1063/1.1957118>.
- Dujardin, E.; T.W. Ebbesen; H. Hiura and K. Tanigaki. (1994).** Capillarity and Wetting of Carbon Nanotubes. *Science* (265), 1850, <https://doi.org/10.1126/science.265.5180.1850>.
- Guillon, O.; J. Gonzalez-Julian; B.Dargatz; T. Kessel, G.Schierning; J.Räthel and M. Herrmann, (2020).** Field-Assisted Sintering Technology/Spark Plasma Sintering: Mechanisms, Materials, and Technology Developments. *Advanced Engineering Materials*, (16), 830-849, <https://doi.org/10.1002/adem.201300409>.

- Guo, B.; M. Song; J. Yi; S. Ni; T. Shen and Y. Du. (2017).** Improving the mechanical properties of carbon nanotubes reinforced pure aluminum matrix composites by achieving non-equilibrium interface. *Materials & Design*, (120), 56-65, <https://doi.org/10.1016/j.matdes.2017.01.096>.
- Hemlata; P. R. Meena; A. P. Singh and K. K. Tejavath. (2020).** Biosynthesis of silver nanoparticles using *Cucumis prophetarum* aqueous leaf extract and their antibacterial and antiproliferative activity against cancer cell lines. *ACS omega*, 5(10), 5520-5528.
- Irhayyim, S.S.; S.R.Ahmed and A.A. Annaz. (2019).** Mechanical performance of micro-Cu and nano-Ag reinforced Al-CNT composite prepared by powder metallurgy technique. *Materials Research Express*, 6, 105071, <https://doi.org/10.1088/2053-1591/ab3b21>.
- Jyoti, K.; M. Baunthiyal and Singh. (2016).** Characterization of silver nanoparticles synthesized using *Urtica dioica* Linn. leaves and their synergistic effects with antibiotics. *Journal of Radiation Research and Applied Sciences* (9), 217-227, <https://doi.org/10.1016/j.jrras.2015.10.002>.
- Kawecki, A.; T. Knych; A. Mamala; P. Kwaśniewski; G. Kiesiewicz; E. Sieja-Smaga; W. Ścieżor; M. Gnielczyk and R. Kowal. (2016).** New Al-Ag Alloys for Electrical Conductors with Increased Current Carrying Capacity. *Archives of Metallurgy and Materials* (61), 1875-1880, <https://doi.org/10.1515/amm-2016-0302>.
- Mansoor, M. and Shahid, M. (2016).** Carbon nanotube-reinforced aluminum composite produced by induction melting. *Journal of applied research and technology*, (14), 215-224, <https://doi.org/10.1016/j.jart.2016.05.002>
- Mohammed, S.M.A.K. and Chen, D.L. (2020).** Carbon Nanotube-Reinforced Aluminum Matrix Composites. *Advanced Engineering Materials*, (22), 1901176, <https://doi.org/10.1002/adem.201901176>.
- Nilagiri, B.; K.B. Ramesh and T. Role. (2018).** Effect and influences of micro and nano-fillers on various properties of polymer matrix composites for microelectronics: A review. *Polym. Adv. Technol.* (29), 1568-1585, <https://doi.org/10.1002/pat.4280>
- Park, S.H.; J. Hwang; G.S. Park; J.H.Ha; M. Zhang; D. Kim; D.J. Yun; S.Lee and S.H. Lee. (2019).** Modeling the electrical resistivity of polymer composites with segregated structures. *Nature Communications* (10), 2537, <https://doi.org/10.1038/s41467-019-10514-4>
- Selvakumar, N. and Gangatharan, K. (2016).** Electrical Resistivity, Tribological Behaviour of Multiwalled Carbon Nanotubes and Nanoboron Carbide Particles Reinforced Copper Hybrid Composites for Pantograph Application. *Advances in Materials Science and Engineering*, 3432979, <https://doi.org/10.1155/2016/3432979>
- Simões, S.; F. Viana; M.A.L Reis and M.F. Vieira. (2015).** Influence of dispersion/mixture time on mechanical properties of Al-CNTs nanocomposites. *Composite Structures*, (126), 114-122, <https://doi.org/10.1016/j.compstruct.2015.02.062>.
- Sharma, M.; H. Pal and V. Sharma. (2014).** Electrical conductivity and thermal expansion measurement of nanocrystalline aluminum reinforced with functionalized multiwall carbon nanotubes. *International Journal of ChemTech Research*, (6), 2057.
- Shin, S.E.; H.J. Choi; J.Y. Hwang and D.H. Bae. (2015).** Strengthening behavior of carbon/metal nanocomposites. *Scientific Reports* (5), 16114, <https://doi.org/10.1038/srep16114>.
- So, K.P.; I.H. Lee; D.L. Duong; T.H. Kim; S.C. Lim; K.H. An and Y.H. Lee. (2011).** Improving the wettability of aluminum on carbon nanotubes. *Acta Materialia* (59), 3313-3320, <https://doi.org/10.1016/j.actamat.2011.01.061>.
- Ujah, C.O.; A.P.I. Popoola; O. Popoola.; V.S.Aigbodion and P. Oladijo. (2020a).** Improving tribological and thermal properties of Al alloy using CNTs and Nb nanopowder via SPS for power transmission conductor. *Transactions of Nonferrous Metals Society of China*, (30), 333-343, [https://doi.org/10.1016/S1003-6326\(20\)65216-5](https://doi.org/10.1016/S1003-6326(20)65216-5).
- Ujah, C.O.; A.P.I. Popoola; O. Popoola and V.S. Aigbodion. (2020b).** Influence of CNTs addition on the mechanical, microstructural, and corrosion properties of Al alloy using spark plasma sintering technique. *The International Journal of Advanced Manufacturing Technology*, (106), 2961-2969, <https://doi.org/10.1007/s00170-019-04699-7>
- Ujah C.O.; V.S. Aigbodion; I.C. Ezema and M.E. Makhatha. (2020c).** Spark Plasma Sintering Of Aluminium Composites- A Review, *J. of Advan. Manufact. Techno.* in press, DOI: 10.1007/s00170-020-06480.
- Ujah, C.O.; A.P.I. Popoola, P.; O. Popoola and V.S. Aigbodion. (2019a).** Enhanced mechanical, electrical and corrosion characteristics of Al-CNTs-Nb composite processed via spark plasma sintering for conductor core. *Journal of Composite Materials*. (53), 3775-3786, <https://doi.org/10.1177/0021998319848055>.
- Ujah, C.O.; A.P.I. Popoola; O. Popoola and V.S. Aigbodion. (2019b).** Enhanced tribology, thermal and electrical properties of Al-CNT composite processed via spark plasma sintering for transmission conductor. *Journal of Materials Science* 2019, 54, 14064-14073, <https://doi.org/10.1007/s10853-019-03894-x>.
- Ujah, C.O.; A.P.I. Popoola; O. Popoola and V.S.Aigbodion. (2019c).** Modification of Al alloy nanopowder with Nb nanopowder on its thermal and tribological properties with SPS for power conductors. *Materials Research Express*, (6), 116592, <https://doi.org/10.1088/2053-1591/ab4be7>.
- Ujah, C.O.; A.P.I. Popoola; O. Popoola and V.S.Aigbodion. (2019d).** Electrical conductivity, mechanical strength and corrosion characteristics of spark plasma sintered Al-Nb nanocomposite. *The International Journal of Advanced Manufacturing Technology*, (101), 2275-2282, <https://doi.org/10.1007/s00170-018-3128-x>.
- Ujah, C.O.; A.P.I. Popoola; O. Popoola and V.S.Aigbodion. (2019e).** Optimisation of spark plasma sintering parameters of Al-CNTs-Nb nano-composite using Taguchi Design of Experiment. *The International Journal of Advanced Manufacturing Technology* (100), 1563-1573, <https://doi.org/10.1007/s00170-018-2705-3>.
- Yuan, C.; Z. Tan; G. Fan; M. Chen; Q. Zheng and Z. Li. (2019).** Fabrication and mechanical properties of CNT/Al composites via shift-speed ball milling and hot-rolling. *J.*

Mater. Res. (34), 2609-2619,  
<https://doi.org/10.1557/jmr.2019.219>

**Zhao, Z.Y.; W.J. Zhao; P.K.Bai; L.Y.Wu and P.C. Huo. (2019).** The interfacial structure of Al/Al<sub>4</sub>C<sub>3</sub> in graphene/Al composites prepared by selective laser melting: First-principles and experimental. *Materials Letters* (255), 126559, <https://doi.org/10.1016/j.matlet.2019.126559>.

**Zhang, X.M.; X.L.Yang and K.Y. Wang. (2019).** Electrical Conductivity Enhancement of Epoxy by Hybrid Carbon Nanotubes and Self-made Silver Nanoparticles. *Fibers and Polymers*, (20), 1480-1485,  
<https://doi.org/10.1007/s12221-019-8640-6>.